# Structure of $N=85$ nuclei within the cluster-phonon coupling model

H. Dias
*Centro Técnico Aeroespacial, Instituto de Atividades Espaciais, Divisao de Estudos Avancados, 12200, San José dos Campos, Sao Paulo, Brasil*

F. Krmpotić
*Departamento de Física, Facultad de Ciencias Exactas, Universidad Nacional de La Plata, 1900 La Plata, Argentina and Departamento de Física Nuclear, Instituto de Física, Universidade de São Paulo, 05508 Sao Paulo, Brasil*

(Received 27 May 1981)

The structure of the low-lying levels in $N=85$ nuclei is discussed in the framework of the cluster-phonon coupling model. Excitation energies, one body reaction amplitudes, dipole and quadrupole moments, and $B(M1)$ and $B(E2)$ values are calculated and compared with the available experimental data.

[ NUCLEAR STRUCTURE $^{143}$Ce, $^{145}$Nd, $^{147}$Sm, and $^{149}$Gd; calculated energy levels, $S$, $Q$, $\mu$, $B(E2)$, and $B(M1)$. Cluster-phonon coupling model. ]

## I. INTRODUCTION

There is abundant experimental evidence for a phase transition, from spherical to permanently deformed nuclei, in the mass region of $A\simeq150$. It can be found in the evolution of: (i) the low energy specta, (ii) the $B(E2)$ values, (iii) the giant dipole resonances, and (iv) the binding energies $B_{2n}$, of the nuclei in question.[1] As a consequence, the nuclei with a few valence neutrons above the $N=82$ major shell should exhibit a very rich variety of nuclear phenomena due to the interplay of fundamental modes of motion, i.e., the single particle excitations, vibrations, and rotations. Such a situation is very appropriate for exploring different coupling between the elementary modes of excitations and several zeroth order symmetries.

The recent calculations, performed within the cluster-vibrator model (CVM), by Heyde *et al.*[2] and by Vanden-Berghe,[3] clearly show that the coexistence of a spherical shell model with quadrupole and octupole vibrations is the dominant ingredient in creating the properties of nuclei with $N=83$ and $N=84$. The aim of the present study is to analyze to which extent the same coupling scheme might be applied to $N=85$ nuclei.

The CVM is a semiphenomenological model based on the assumption that the low-lying nuclear states can be described in terms of a cluster of valence fermions (particles or quasiparticles) and a quadrupole and/or an octupole vibrational field. The residual interactions among the particles is usually approximated by a pairing force and all other correlations are averaged and included into the model through an effective vibrator, effective charges, and renormalized single-particle energies. This framework has been extensively used ever since it was suggested by Bohr and Mottelson[4] and extended and developed by Raz,[5] Alaga,[6] and Kisslinger and Sorensen.[7]

During the last few years several experimental studies of $N=85$ isotones have been performed, which provide data on the spectra, electromagnetic properties, and high-spin states.[8–15] However, the experimental information for these nuclei is far from complete, even for the low-lying states.[8–15] Most of the existing data for the low-energy spectra and one particle spectroscopic strengths for $^{143}$Ce, $^{145}$Nd, $^{147}$Sm, and $^{149}$Gd nuclei are shown in Fig. 1.

When the present work was initiated the theoretical studies of the $N=85$ nuclei were also quite limited. The only calculations available in the litera-

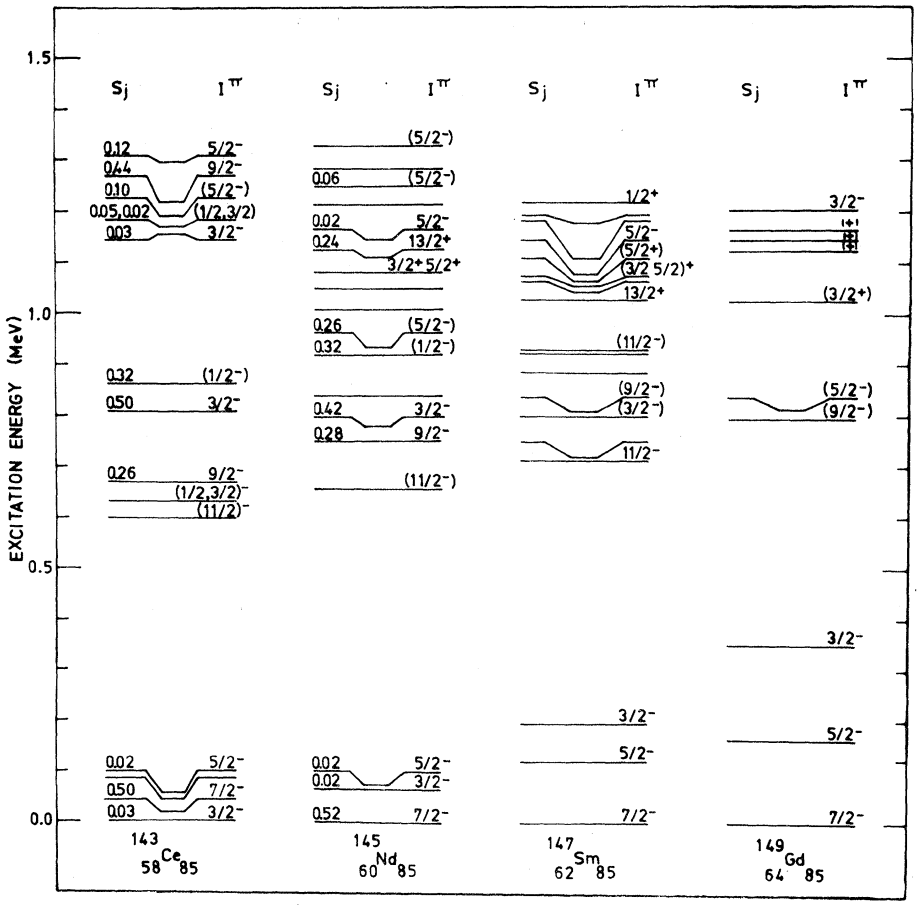


FIG. 1. The experimental energy spectra and the $(d,p)$ stripping strengths for $N=85$ nuclei (Refs. 8–15).

ture were those of: (i) Kisslinger and Sorensen,[7] who described a few properites of $^{145}$Nd and $^{147}$Sm nuclei by means of the quasiparticle-core coupling model; and (ii) Garret *et al.*,[16] who interpreted several low lying collective states and the high spin band structure in the $^{147}$Sm nucleus by coupling the $(2f_{7/2})^3$ cluster to a harmonic quadrupole vibrator.

The present calculations include more correlations than the above mentioned theoretical studies. With respect to the first one, we include explicitly: (a) the Pauli principle in the valence shell, (b) the anharmonic structure of the neighboring doubly-even nuclei, and (c) the effect of broken and promoted pairs. With respect to the second, we consider the interplay of the vibrational field with all three-particle clusters built up from the single particle orbits in the $N=82$ major shell, and not only with the $(2f_{7/2})^3$ cluster. In other words, although we employ the same dynamics (Alaga model) as Garret *et al.*,[16] our wave functions will be more correlated since we use a more complete kinematics.

While the present work was in progress, three different studies of the $N=85$ nuclei, in the framework of the CVM model, were published.[13,14,17] However, in all these works attention was paid only to isolated aspects of the nuclei in question, namely to: (1) energy spectra in $^{147}$Sm (Ref. 13), (2) $B(E2)$ values in $^{147}$Sm (Ref. 14), and (3) the $^{142}$Ce$(d,p)$ reaction (Ref. 17).

It is worth noting that all medium and heavy nuclei with one open shell and three valence particles or holes have been extensively analyzed, so far, within the Alaga model,[18–39] with the exception of the $N=85$ nuclei.

## II. FORMALISM

A detailed description of the CVM can be found in the literature.[17–39] Here, only the main formulas will be given in order to establish the notation. The total Hamiltonian is

$$H = H_0 + H_{\rm res} + H_{\rm int} , \tag{1}$$

where $H_0$ represents the energy of the unperturbed system consisting of quadrupole and octupole vibrational fields and valence neutrons in a central field. The residual interaction energy among the neutrons in the shell-model cluster, $H_{\rm res}$, only includes explicitly the pairing force. The interaction energy between the $p$-particle cluster and the vibrational fields is given by the expression

$$H_{\rm int} = -\sum_{\lambda=2}^{3} \frac{\beta_\lambda}{(2\lambda+1)^{1/2}} \sum_{\mu=-\lambda}^{\lambda} \left[ b_\lambda^{\mu +} + (-1)^{\lambda-\mu} b_\lambda^{-\mu} \right] \sum_{i=1}^{p} k(r_i) Y^*_{\lambda\mu}(\phi_i \theta_i) , \tag{2}$$

where $\beta_\lambda$ are the deformation parameters and all other symbols have the standard meaning.[38] The deformation parameter $\beta_2$ is related to coupling strength $a$, used in the previous calculations,[18–24] by $a = \langle K \rangle \beta_2 / \sqrt{20\pi}$.

The Hamiltonian (1) is diagonalized in the basis

$$|(j_1 j_2) J_{12}, R; I\rangle \equiv |\chi_2; I\rangle$$

for the $N=84$ nuclei ($p=2$) and in the basis

$$|(j_1 j_2) J_{12}, j_3 J, R; I\rangle \equiv |\chi_3; I\rangle$$

for the $N=85$ nuclei ($p=3$). Here the symbol $R$ stands for the quantum numbers $\{N_2 R_2, N_3 R_3, R\}$, where $N_\lambda$ is the number of $\lambda$-pole phonons of angular momentum $\vec{\rm R}_\lambda$ and $\vec{\rm R} = \vec{\rm R}_2 + \vec{\rm R}_3$. In the case of $(j^3)\,J$ configuration with $j \geq \frac{7}{2}$, an additional quantum number is introduced. The corresponding wave functions read

$$|I_m\rangle = \sum_{\{\chi_2\}} \eta_2(\chi_2; I_m) |\chi_2; I\rangle$$

and

$$|I_n\rangle = \sum_{\{\chi_3\}} \eta_3(\chi_3; I_n) |\chi_3; I\rangle ,$$

where the subindices $m$ and $n$ distinguish between states of same angular momentum.

The parentage coefficient, which measures to which extent the nuclear state $|I_n\rangle$ can be built up by adding a nucleon in the single particle state $lj$ to the core state $|I_m\rangle$, is given by

$$\begin{aligned}\theta(lj, I_m, I_n) &= \langle I_n || a_{lj}^+ || I_m \rangle (2I_n+1)^{-1/2} \\ &= \sum_{\{\chi_2'\},\{\chi_3\}} (-)^{I_m + j + R + J} (2I_m+1)^{1/2} \langle (j_1 j_2) J_{12} j_3 J || a_{lj}^+ || (j_1' j_2') J_{12}' \rangle \\ &\quad \times \begin{Bmatrix} j & J_{12} & J \\ R & I_n & I_m \end{Bmatrix} \eta_2(\chi_2'; I_m) \eta_3(\chi_3; I_n) \delta_{RR'} .\end{aligned} \tag{3}$$

The quantities $\theta(l_j, I_m; I_n)$ satisfy the sum rule

$$\sum_{l,j,I_m} |\theta(lj, I_m; I_n)|^2 = 3 . \tag{4}$$

The spectroscopic factor for a stripping process, i.e, for forming the state $|I_n\rangle$ by transferring a particle to the orbital $lj$ of the target state $|0_1\rangle$, reads

$$S(lj, I_n) = |\theta(lj, 0_1; I_n)|^2 . \tag{5}$$

The electric quadrupole and magnetic-dipole operators consist of a particle and a collective part

$$\begin{aligned}\mathcal{M}(E2,\mu) &= e_n^{\rm eff} \sum_{i=1}^{p} r_i^2 Y_{2\mu}(\phi_i, \theta_i) \\ &\quad + \frac{3R_0^2}{4\pi} e_v^{\rm eff} \left[ b_2^{\mu +} + (-1)^\mu b_2^{-\mu} \right] ,\end{aligned} \tag{6}$$

$$\mathcal{M}(M1,\mu) = \left[ \frac{3}{4\pi} \right]^{1/2} \left[ g_R R_\mu + g_l L_\mu + g_s S_\mu \right] \mu_N , \tag{7}$$

where $e_n^{\rm eff}$ is the effective neutron charge, $e_v^{\rm eff} = Ze\beta_2/\sqrt{5}$ is the effective vibrator charge, and $g_R$, $g_l$, and $g_s$ are, respectively, the collective, orbital, and spin gyromagnetic ratios.

## III. CALCULATIONS

Our starting point in the choice of model parameters were the experimental and theoretical studies performed so far on $N=82$, $N=83$, and $N=84$ nuclei.[2,3,7,40–44] Namely, we took:

(i) the centroid energies, measured in the

$^{144}$Sm$(d,p)$ reaction study[40] as the single particle energies $\epsilon(j)$;

(ii) the effective quadrupole phonon energy $\hbar\omega_2$ used in the calculation of $N=84$ nuclei[3];

(iii) the excitation energy of the $3_1^-$ state in $^{142}$Nd (Ref. 42) for the effective octupole phonon energy $\hbar\omega_3$;

(iv) the quadrupole deformation parameter $\beta_2$ measured in the ($^{16}$O,$^{16}$O′) reaction on $^{142}$Nd (Ref. 42) and adopted by Nuclear Data Sheets[43];

(v) the octupole deformation parameter $\beta_3$ from the $(\alpha,\alpha')$ experiment on $^{142}$Nd (Ref. 44); and

(vi) the usual pairing strength ($G\simeq 24/A$) for the pairing interaction.[7] The numerical values for the parameters selected in this way are listed in the first column of Table I (parametrization I).

The radial matrix elements $\langle j_2 | k(r) | j_1 \rangle$ and $\langle j_2 | r^2 | j_1 \rangle$ were calculated numerically using the wave functions obtained from the Woods-Saxon potential[45] and their values are displayed in Table II.[46]

The size of the configuration space was fixed by the conditions

$$\epsilon(j_1)+\epsilon(j_2)+N_2\hbar\omega_2+N_3\hbar\omega_3 \leq \begin{cases} 4.5 \text{ MeV} & \text{for } J_{12}\neq 0 \\ 4.5 \text{ MeV}+\dfrac{G}{2}(2j_1+1) & \text{for } J_{12}=0 \end{cases} \tag{8a}$$

and

$$\epsilon(j_1)+\epsilon(j_2)+\epsilon(j_3)+N_2\hbar\omega_2+N_3\hbar\omega_3 \leq \begin{cases} 3.5 \text{ MeV} & \text{for } J_{12}\neq 0 \\ 3.5 \text{ MeV}+\dfrac{G}{2}(2j_1+1) & \text{for } J_{12}=0 \end{cases} \tag{8b}$$

for $N=84$ and $N=85$ nuclei, respectively. The number of phonons in both cases was $N_2\leq 3$ and $N_3\leq 1$. In this way we still have reasonable dimensions for the energy matrices while retaining the most important basic states.

The electromagnetic properties were evaluated with the usual values of the electromagnetic electric charge and the effective gyromagnetic ratios, namely:

$$e_n^{\text{eff}}=0.5e \ ; \ e_v^{\text{eff}}=\frac{\beta_2 Ze}{\sqrt{5}}=3.1e \ ,$$
$$g_R=Z/A=0.41 \ ; \ g_l=0 \ ; \ g_s^{\text{eff}}=0.5g_s^{\text{free}}=-1.91 \ . \tag{9}$$

TABLE I. Model parameters used in the present calculation and chosen as explained in the text.

| | I | II | III | IV |
|---|---|---|---|---|
| $\epsilon(2f_{7/2})$ (MeV) | 0.00 | 0.00 | 0.00 | 0.00 |
| $\epsilon(1h_{9/2})$ (MeV) | 1.37 | 1.37 | 0.50 | 0.50 |
| $\epsilon(3p_{3/2})$ (MeV) | 1.07 | 1.07 | 1.50 | 2.00 |
| $\epsilon(3p_{1/2})$ (MeV) | 1.88 | 1.88 | 1.30 | 1.30 |
| $\epsilon(2f_{5/2})$ (MeV) | 1.94 | 1.94 | 0.90 | 0.90 |
| $\epsilon(1i_{13/2})$ (MeV) | 1.49 | 1.49 | 0.70 | 0.70 |
| $\hbar\omega_2$ (MeV) | 1.20 | 1.20 | 1.20 | 1.20 |
| $\beta_2$ | 0.115 | 0.115 | 0.115 | 0.10 |
| $\hbar\omega_3$ (MeV) | 2.08 | 2.08 | 2.08 | 2.08 |
| $\beta_3$ | 0.14 | 0.14 | 0.14 | 0.14 |
| $G$ (pairing) (MeV) | 0.15 | 0.10 | 0.10 | 0.10 |

TABLE II. Matrix elements of the radial form factors $k(r)=-r(dV/dr)$ and $r^2$. A Woods-Saxon single-particle potential was used with parameters $V_0=49.4$ MeV, $R_0=1.25\,A^{1/3}$ fm ($A=145$), $a_0=0.59$ fm, and $\lambda_{s.o.}=30$ MeV.

| $n_2l_2j_2$ | $n_1l_1j_1$ | $\langle n_2l_2j_2 \mid k(r) \mid n_1l_1j_1\rangle$ (MeV) | $\langle n_2l_2j_2 \mid r^2 \mid n_1l_1j_1\rangle$ (fm$^2$) |
|---|---|---|---|
| $2f\frac{7}{2}$ | $2f\frac{7}{2}$ | 55.9 | 31.1 |
| | $1h\frac{9}{2}$ | 44.8 | 15.9 |
| | $3p\frac{3}{2}$ | 50.9 | 29.4 |
| | $2f\frac{5}{2}$ | 56.1 | 31.5 |
| | $1i\frac{13}{2}$ | 58.9 | |
| $1h\frac{9}{2}$ | $1h\frac{9}{2}$ | 52.4 | 28.8 |
| | $2f\frac{5}{2}$ | 47.2 | 18.3 |
| | $1i\frac{13}{2}$ | 61.3 | |
| $3p\frac{3}{2}$ | $3p\frac{3}{2}$ | 50.0 | 35.7 |
| | $3p\frac{1}{2}$ | 50.1 | 36.8 |
| | $2f\frac{5}{2}$ | 50.2 | 29.9 |
| $2f\frac{5}{2}$ | $2f\frac{5}{2}$ | 56.6 | 32.6 |
| | $3p\frac{1}{2}$ | 50.9 | 31.2 |
| | $1i\frac{13}{2}$ | 61.0 | |
| $1i\frac{13}{2}$ | $1i\frac{13}{2}$ | 74.2 | 34.8 |

## III. RESULTS AND DISCUSSION

### A. Energy spectra and spectroscopic amplitudes

The measured spectra for $^{143}$Ce (Refs. 8 and 11), $^{145}$Nd (Refs. 9 and 10), $^{147}$Sm (Refs. 12–14), and $^{149}$Gd (Ref. 15), together with the one-particle $(d,p)$ spectroscopic strengths for $^{143}$Ce (Ref. 47) and $^{145}$Nd (Ref. 48) nuclei are shown in Fig. 1.

From the energy splittings of the $\frac{3}{2}^-_1$, $\frac{5}{2}^-_1$, and $\frac{7}{2}^-_1$ states one is led to the conclusion that the anharmonicity effects decrease in going from $^{143}$Ce ($Z=58$) to $^{149}$Gd ($Z=64$), i.e., in approaching the transitional region. This somewhat surprising fact is consistent, however, with the variation of the first excited $2^+$ states in $N=82$ nuclei and suggests the existence of an unusually large energy gap at $Z=64$, between the proton $g_{7/2}$ and $d_{5/2}$ orbitals and the $h_{11/2}$ state.[49,50]

Initially, the calculations were performed with constant values for the radial matrix elements [$\langle k(r)\rangle=50$ MeV and $\langle r^2\rangle=\frac{3}{5}(1.2A^{1/3})^2$fm$^2$] and only quadrupole phonons were considered. These calculations yielded a reasonable description for most of the properties of the $N=85$ isotones (energy spectra, electromagnetic transitions and moments, the parentage coefficients of the $\frac{7}{2}^-_1$ and $\frac{3}{2}^-_2$ resonances in $^{145}$Nd, the spectroscopic factors of the low-lying triplet $\frac{3}{2}^-_1$, $\frac{5}{2}^-_1$, and $\frac{7}{2}^-_1$ in $^{143}$Ce and $^{145}$Nd, and the pickup spectroscopic amplitudes in $^{147}$Sm).

Moreover, it was easy to understand the variation of the energy spectra, i.e., the increase in the energy splittings between the $\frac{3}{2}^-_1$, $\frac{5}{2}^-_1$, and $\frac{7}{2}^-_1$ states, in going from $^{143}$Ce to $^{149}$Gd. This could be done either by smoothly diminishing the anharmonicity effects generated by the CVM (decreasing the deformation parameter $\beta_2$ and/or increasing the phonon energy $\hbar\omega_2$), or by smoothly increasing the pairing strength $G$.

By optimizing the collective parameters $\hbar\omega_\lambda$ and $\beta_\lambda$ and the pairing strength $G$ it was not possible to account for the distribution of the spectroscopic strengths seen experimentally in $^{143}$Ce and $^{145}$Nd nuclei, in the energy region between 0.6 and 1.5 MeV. Van der Berghe and Paar[17] faced the same problem in their study of the $^{142}$Ce$(d,p)^{143}$Ce reac-

tion. The parametrization employed by them is close to our parametrization I, and their configuration space is also similar to the one used by us. (Our single-particle energies are all about 200 keV different from those employed in Ref. 17, but, qualitatively, this difference is not important at all.) To a certain extent, they were able to surmount this difficulty by including higher multiplet states (but a smaller number of single-particle states).

We have attacked the problem differently, and tried some additional correlations which are not usually considered in the three-particle-cluster model (Alaga model), but which might, in principle, play an important role in the description of low-lying states. Explicitly, (i) instead of using constant values for the form factors $\langle k(r)\rangle$ and $\langle r^2\rangle$, we have employed those given in Table II, which were obtained from the Woods-Saxon potential; (ii) in addition to the quadrupole phonons, we have also included an octupole phonon; and (iii) the pairing force was substituted by the surface delta interaction. It turned out that none of these effects was able to lower the states with spin and parity $\frac{9}{2}^-$, $\frac{1}{2}^-$, and $\frac{5}{2}^-$ and with large spectroscopic factors into the energy region where they have been observed experimentally. In view of this situation, a thorough study of the spectroscopic factors as a function of the model parameters was done. A few relevant results are discussed below.

Although the properties of the low-lying states do not become qualitatively altered by the above mentioned correlations, we prefer to present the final results with modifications (i) and (ii) included. On the other hand, modification (iii) was left out owing to the fact that the numerical calculation of the residual interaction between broken pairs ($J_{12}\neq 0$) was rather time consuming. It is worth noticing that the single-particle energies when evaluated with the Woods-Saxon potential are all about 0.5 to 1.0 MeV higher than those taken from the experiment and used in the present calculations.

In Fig. 2 the calculated energy spectra and the one particle transfer strengths are shown. The energies of the $\frac{7}{2}_1^-$, $\frac{3}{2}_1^-$, $\frac{5}{2}_1^-$, $\frac{11}{2}_1^-$, and $\frac{3}{2}_2^-$ states in $^{145}$Nd are fairly well reproduced by the calculations with parametrization I [Fig. 2(a)]. The wave functions of these states, are of a rather mixed character. The states $\frac{7}{2}_1^-$ and $\frac{3}{2}_2^-$ are based, in zeroth order approximation, on the zero phonon clusters $|\{(f_{7/2})^3\}J=\frac{7}{2}\rangle$ and $|\{(f_{7/2})^2 0,p_{3/2}\}J=\frac{3}{2}\rangle$, respectively. The remaining states exhibit a pronounced collective character, with the dominant components

$$|\{(f_{7/2})^3\}J=\tfrac{7}{2},12;I=\tfrac{3}{2},\tfrac{5}{2},\tfrac{9}{2},\tfrac{11}{2}\rangle$$

and

$$|\{(f_{7/2})^3\}J,00;\tfrac{3}{2},\tfrac{5}{2},\tfrac{7}{2},\tfrac{9}{2},\tfrac{11}{2}\rangle\ .$$

The relative position of this group of levels is mainly governed by the pairing force, which lowers the seniority one states, and by the quadrupole vibrational field, which strongly pushes down the $\frac{3}{2}_1^-$ and $\frac{5}{2}_1^-$ states. The mechanisms which bring these two states close to the $\frac{7}{2}_1^-$ state are different. The lowering of the $\frac{3}{2}_1^-$ state mainly arises because of the single-particle cluster $|\{(f_{7/2})^2 0,p_{3/2}\}J=\frac{3}{2}\rangle$ lying close the zeroth order component $|\{(f_{7/2})^3\tfrac{7}{2},12;\tfrac{3}{2}\rangle$. In the second case the origin of the effect stems from the Pauli principle through the recoupling

$$\begin{Bmatrix} \frac{7}{2} & \frac{7}{2} & 2 \\ \frac{7}{2} & J & 2 \end{Bmatrix},$$

which is positive for $J=\frac{5}{2}$ and negative for all other values of $J$.

The energy ordering $\frac{3}{2}_1^-$, $\frac{7}{2}_1^-$, $\frac{5}{2}_1^-$, exhibited by the lowest states in $^{143}$Ce, can be accounted for in the calculation either by increasing the deformation or by diminishing the pairing interaction. The last possibility is illustrated by Fig. 2(b), where we used a pairing strenght of 0.1 MeV instead of 0.15 MeV (parametrization II). The remaining states are influenced by this change in parametrization only very weakly.

In Ref. 47 an additional low lying $l=1$ state (at 0.056 MeV) in $^{143}$Ce was reported. Within the framework of the model employed here it is not possible to obtain such a state. It should be mentioned, however, that the experimental evidences for the existence of this level are very weak.[11] In addition, in the energy region between 0.5 and 1 MeV, of the experimentally known six or seven levels in $^{143}$Ce, $^{145}$Nd, and $^{147}$Sm, the theory is able to account only for three or four states. The remaining levels probably arise from the 1 hole-4 particle clusters, involving $s_{1/2}{}^{-1}$, $d_{3/2}{}^{-1}$, and $h_{11/2}{}^{-1}$ neutron holes.

Among the calculated spectroscopic factors of the low-lying triplet, only that of the $\frac{7}{2}_1^-$ agrees with the measured values in $^{143}$Ce and $^{145}$Nd. The concordance between the theory and experiment for the remaining two states is only qualitative.

In the energy region between 0.6 and 1.5 MeV

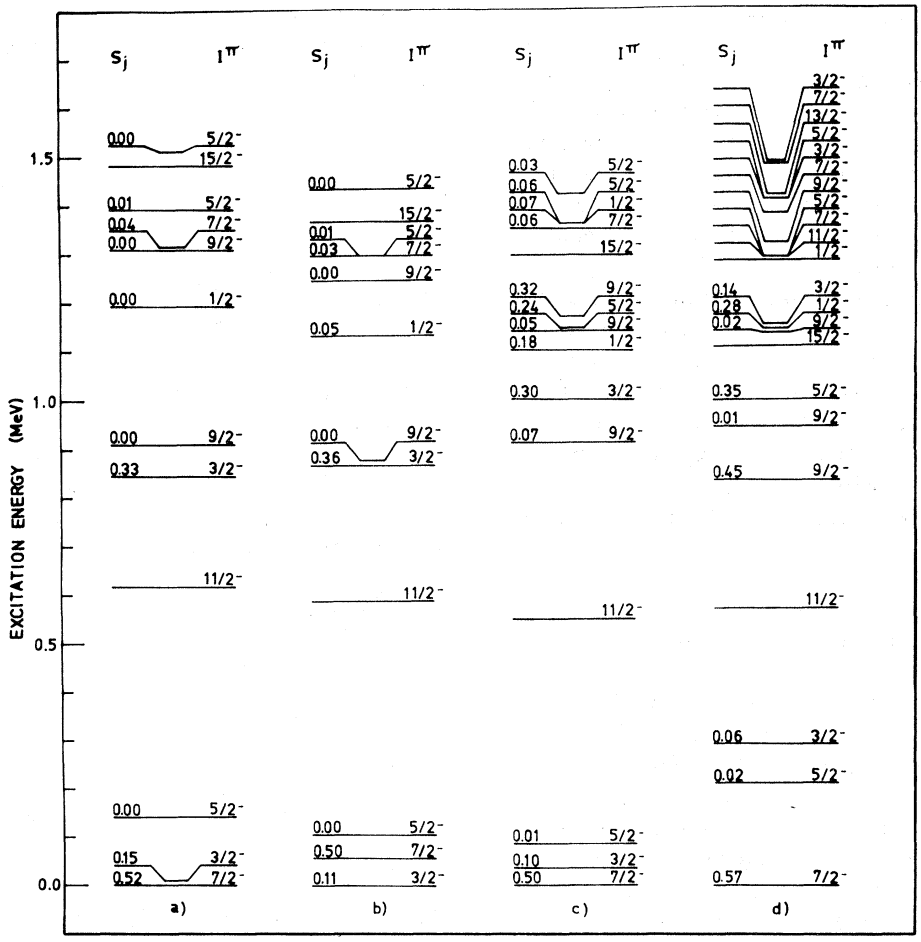


FIG. 2. The calculated energy levels and reaction strengths for the negative-parity states in $N=85$ nuclei. The spectra (a), (b), (c), and (d) correspond to parametrizations I, II, III, and IV, respectively.

most of the reaction strength, observed experimentally in $^{143}$Ce and $^{145}$Nd nuclei, is missed in the theoretical description when we use the parameters extracted from the experimental data (parametrization I or II); only the spectroscopic factor of the $\frac{3}{2}_2^-$ state is reasonably well reproduced by theory in this energy region [see Figs. 2(a) and (b)]. The most pronounced discrepancy between the theory and the experimental data appears in the energy distribution of the $l=5$ strength; experimentally, two $\frac{9}{2}$ states with large spectroscopic factors and with energy excitation below 1.5 MeV in both $^{143}$Ce and $^{145}$Nd nuclei have been reported, while the lowest calculated $\frac{9}{2}$ state with large spectroscopic strength lies at 2.1 MeV.

From the study of several different parametrizations it was possible to conclude that the lowering in energy of the $l=5$ strength within the configuration space given by condition (8) could be achieved only by diminishing the single particle energy of the $h_{9/2}$ state with a simultaneous increase of the energy of the orbital $p_{3/2}$. Moreover, it was necessary to lower the single-particle energies at the $p_{1/2}$ and $f_{5/2}$ states in order to transfer a reasonable amount of the spectroscopic strength into the states $\frac{1}{2}_1^-$ and $\frac{5}{2}_1^-$, respectively. One of the calculations which reproduces the measured energy spectra and the spectroscopic factors in $^{143}$Ce and $^{145}$Nd nuclei fairly well is that performed with parametrization III. The corresponding results are displayed in Fig. 2(c). The results obtained with parametrization IV [which are shown in Fig. 2(d)], illustrate: (i) to which extent the distribution of the $l=5$ strength depends on the position of the $p_{3/2}$ orbital, and (ii) in what manner the energy splittings between the $\frac{3}{2}_1^-$, $\frac{5}{2}_1^-$, and $\frac{7}{2}_1^-$ levels are increased, when the de-

formation parameter $\beta_2$ decreases.

The experimental results for the spectroscopic factors $S(l)$ measured through the $^{147}$Sm$(d,p)$ reaction by Oelert *et al.*[51] are compared in Table III with the calculation obtained with parametrization I. The agreement is quite reasonable for the $0_1^+$, $4_1^+$, and $6_1^+$ states, while the experimental spectroscopic factors for the first two $2^+$ states are poorly reproduced by the theory.

By the inelastic proton scattering through analog resonances it is possible to measure both the magnitude and the sign of the neutron parentage coefficients $\theta(lj,I_m,I_n)$. Such an experiment was performed recently by Foster[11] on the $\frac{7}{2}^-_1$ and $\frac{3}{2}^-_2$ resonances in $^{145}$Nd. His results, together with our calculated values within parametrization I, are shown in Table IV, with the overall agreement quite satisfactory.

### B. Electromagnetic properties

We limit our attention here to the low-lying states $\frac{7}{2}^-_1$, $\frac{5}{2}^-_1$, $\frac{3}{2}^-_1$, $\frac{11}{2}^-_1$, and $\frac{3}{2}^-_2$, as the wave functions of these levels are rather stable against a relatively small variation of model parameters. The matrix elements of the electromagnetic operators $\mathcal{M}(E2)$ and $\mathcal{M}(M1)$ were evaluated with the wave functions calculated with parametrization I. The main component of these wave functions are listed in Table V. The calculated moments and transition probabilities are compared with the experimental data[9,12,14,52] in Table VI.

When only the first order effects are included, which involves the emission or absorption of a virtual phonon and its interaction with the electromagnetic field, the quadrupole moment for a predominantly particle state is enhanced and given by the expression[53]

$$Q(J)=Q_c(J)e^{\text{eff}}(J)\ , \tag{10}$$

where $Q_c(J)$ is the bare quadrupole moment of the cluster and

$$e^{\text{eff}}(J)=e_n^{\text{eff}}+\frac{3\beta_2{}^2R_0{}^2Ze}{10\pi\hbar\omega_0}\frac{\langle J||kY_2||J\rangle}{\langle J||r^2Y_2||J\rangle}\ . \tag{11}$$

Within parametrization I and radial matrix elements from Table II one has $e^{\text{eff}}(J)=5.01e$ and $e^{\text{eff}}(J)=4.84e$ for the clusters $\{(f_{7/2})^3\}J=\frac{3}{2},\frac{5}{2},\frac{7}{2},\frac{11}{2}$ and $\{(f_{7/2})^2 0,p_{3/2}\}J=\frac{3}{2}$, respectively. Given below are the zeroth order approximations for the low-lying states in question and the corresponding quadrupole moments as obtained from the relation (10)

$$\tfrac{7}{2}^-_1 : |\{(f_{7/2})^3\}\tfrac{7}{2},00;\tfrac{7}{2}\rangle\ ,\quad Q=-0.36\ e\,\text{b}\ ,$$
$$\tfrac{5}{2}^-_1 : |\{(f_{7/2})^3\}\tfrac{5}{2},00;\tfrac{5}{2}\rangle\ ,Q=-0.98\ e\,\text{b}\ ,$$
$$\tfrac{3}{2}^-_1 : |\{(f_{7/2})^3\}\tfrac{3}{2},00;\tfrac{3}{2}\rangle\ ,\quad Q=0.64\ e\,\text{b}\ ,$$
$$\tfrac{11}{2}^-_1 : |\{(f_{7/2})^3\}\tfrac{11}{2},00;\tfrac{11}{2}\rangle\ ,\quad Q=-0.11\ e\,\text{b}\ ,$$
$$\tfrac{3}{2}^-_2 : |\{(f_{7/2})^2 0,p_{3/2}\},00;\tfrac{3}{2}\rangle\ ,\quad Q=-0.69\ e\,\text{b}\ .$$

Comparing these quadrupole moments with the results of the exact calculations shown in Table VI, one can see that the estimate (10) reproduces correctly only the quadrupole moment of the $\frac{7}{2}^-_1$ state. For the remaining states the higher order effects are quite important in establishing the magnitude of the corresponding quadrupole moments.

TABLE III. Comparsion of experimental and theoretical excitation energies and spectroscopic factors $S(l)$ in $^{146}$Sm. The calculation was performed with parametrization I and the experimental data are from the work of Oelert *et al.* (Ref. 51). We abbreviate $S(l,j=l\pm\frac{1}{2},I_m 7/2_1)\equiv|\theta(l,j=l\pm\frac{1}{2},I_m,\frac{7}{2}^-_1)|^2$ as $S(j=l\pm\frac{1}{2})$ and define $S(l)$ as $S(j=l-\frac{1}{2})+S(j=l+\frac{1}{2})$.

| $I_m$ | $E_{\text{exp}}$ (MeV) | $E_{\text{th}}$ (MeV) | $l$ | $S(l)_{\text{exp}}$ | $S(j=l-\frac{1}{2})_{\text{th}}$ | $S(j=l+\frac{1}{2})_{\text{th}}$ | $S(l)_{\text{th}}$ |
|---|---|---|---|---|---|---|---|
| $0_1^+$ | 0 | 0 | 3 | 0.56 | | 0.52 | 0.52 |
| $2_1^+$ | 0.75 | 0.72 | 1 | 0.05 | | 0.02 | 0.02 |
| | | | 3 | 0.14 | 0.00 | 0.04 | 0.04 |
| $4_1^+$ | 1.38 | 1.24 | 1 | | 0.00 | 0.07 | 0.07 |
| | | | 3 | 0.62 | 0.00 | 0.48 | 0.48 |
| $2_2^+$ | 1.65 | 1.52 | 1 | 0.14 | | 0.01 | 0.01 |
| | | | 3 | 0.01 | 0.00 | 0.14 | 0.14 |
| $6_1^+$ | 1.81 | 1.60 | 3 | 0.82 | 0.00 | 0.60 | 0.60 |

TABLE IV. Comparison of theoretical and experimental spectroscopic amplitudes $\theta(1_j,I_m,I_n)$ for the $\frac{7}{2}^-_1$ and $\frac{3}{2}^-_2$ states in $^{145}$Nd. The calculation was performed with parametrization I and the experimental data were provided by Foster (Ref. 11).

| $I_n$ | | $\theta(f_{7/2},I_m,\frac{7}{2}^-_1)$ | $\theta(f_{5/2},I_m,\frac{7}{2}^-_1)$ | $\theta(p_{3/2},I_m,\frac{7}{2}^-_1)$ | $\theta(p_{1/2},I_m,\frac{7}{2}^-_1)$ | $\theta(f_{7/2},I_m,\frac{3}{2}^-_1)$ | $\theta(f_{5/2},I_m,\frac{3}{2}^-_2)$ | $\theta(p_{3/2},I_m,\frac{3}{2}^-_2)$ | $\theta(p_{1/2},I_m,\frac{3}{2}^-_2)$ |
|---|---|---|---|---|---|---|---|---|---|
| th | $0^+_1$ | 0.72 | | | | | | −0.58 | |
| exp | | 0.78 | | | | | | −0.77 | |
| th | $2^+_1$ | −0.20 | 0.06 | 0.14 | | 0.26 | −0.02 | −0.43 | −0.08 |
| exp | | −0.58 | 0.39 | −0.14 | | −0.41 | −0.14 | −0.57 | −0.36 |
| th | $4^+_1$ | −0.69 | 0.02 | −0.27 | 0.01 | −0.21 | 0.00 | | |
| exp | | −0.58 | 0.30 | −0.30 | 0.00 | −0.33 | 0.00 | | |
| th | $2^+_2$ | 0.37 | 0.00 | −0.08 | | 0.44 | 0.00 | 0.04 | −0.05 |
| exp | | 0.56 | 0.00 | −0.10 | | 0.57 | 0.00 | 0.10 | 0.00 |
| th | $6^+_1$ | −0.77 | −0.03 | | | | | | |
| exp | | −0.99 | 0.00 | | | | | | |
| th | $0^+_2$ | 0.04 | | | | | | 0.05 | |
| exp | | 0.28 | | | | | | | |
| th | $2^+_3$ | −0.26 | 0.00 | −0.13 | | 0.60 | 0.03 | 0.06 | 0.03 |
| exp | | −0.55 | 0.00 | 0.07 | | | | | |

In zeroth order all the $E2$ transitions among the above mentioned states are of the particle type $N=0$, $\Delta N=0$. By including first order induced collective contributions, the transition moment $\langle J_f||r^2Y_2||J_i\rangle$ is renormalized by the effective charge

$$e^{\text{eff}}(J_i;J_f)=e_n^{\text{eff}}+\frac{3\beta_2{}^2R_0{}^2Ze}{10\pi\hbar\omega_2}\frac{\langle J_f||kY_2||J_i\rangle}{\langle J_f||r^2Y_2||J_i\rangle}\times\frac{(\hbar\omega_2)^2}{(\hbar\omega_2)^2-(\epsilon_{J_i}-\epsilon_{J_f})^2}\ , \tag{12}$$

where $\epsilon_{J_i}$ and $\epsilon_{J_f}$ are the energies of the cluster in the initial and final state, respectively. As in the present case this effective charge is large ($\simeq 5e$), it is easy to understand, at least qualitatively, the enhancement of the

$$B(E2;\tfrac{7}{2}^-_1\rightarrow\tfrac{5}{2}^-_1)\ ,$$

$$B(E2;\tfrac{7}{2}^-_1\rightarrow\tfrac{3}{2}^-_1)\ ,$$

$$B(E2;\tfrac{7}{2}^-_1\rightarrow\tfrac{11}{2}^-_1)\ ,$$

and

$$B(E2;\tfrac{5}{2}^-_1\rightarrow\tfrac{3}{2}^-_1)$$

values. Within the same approximation the $\frac{5}{2}^-_1\rightarrow\frac{3}{2}^-_1$ and $\frac{3}{2}^-_1\rightarrow\frac{3}{2}^-_2$ $E2$ transitions are forbidden and the calculated results for these transitions, shown in Table VI, arise from the higher order effects. Also in the case of the $\frac{7}{2}^-_1\rightarrow\frac{3}{2}^-_2$ transition, the higher order effects are essential in generating a relatively small $B(E2)$ value.

In the zeroth order only the spin part of the $\mathcal{M}(M1)$ operator contributes to the magnetic dipole moment with the following values:

$$\mu(\tfrac{7}{2}^-_1)=\frac{g_s}{2}=-0.955\ \mu_N\ ,$$

$$\mu(\tfrac{5}{2}^-_1)=(\tfrac{5}{12})^{1/2}\frac{g_s}{2}=-0.616\ \mu_N\ ,$$

$$\mu(\tfrac{3}{2}^-_1)=(\tfrac{5}{42})^{1/2}\frac{g_s}{2}=-0.330\ \mu_N\ ,$$

$$\mu(\tfrac{11}{2}^-_1)=(\tfrac{143}{42})^{1/2}\frac{g_s}{2}=-1.762\ \mu_N\ ,$$

$$\mu(\tfrac{3}{2}^-_2)=\frac{g_s}{2}=-0.955\ \mu_N\ .$$

After including the cluster-field interaction the magnetic moments turn out to be the following: $\mu(\frac{7}{2}^-_1)=-0.897\ \mu_N$, $\mu(\frac{5}{2}^-_1)=-0.586\ \mu_N$,

TABLE V. Calculated wave functions for the low-lying states of the $N=85$ nuclei. Each state is denoted by its spin, parity, and order of appearance. The parameters used are given in the first column of Table I. Only those amplitudes that contribute more than 4% are listed.

$$|(\tfrac{3}{2}^-)_1\rangle = -0.34\,|\{(f\tfrac{7}{2})^3\}\tfrac{3}{2};00\rangle - 0.30\,|\{(f\tfrac{7}{2})^2 0, p\tfrac{3}{2}\}\tfrac{3}{2};00\rangle$$
$$+0.28\,|\{(f\tfrac{7}{2})^2 2, p\tfrac{3}{2}\}\tfrac{3}{2};00\rangle + 0.26\,|\{(f\tfrac{7}{2})^3\}\tfrac{5}{2};12\rangle$$
$$-0.20\,|\{(f\tfrac{7}{2})^2 4, p\tfrac{3}{2}\}\tfrac{5}{2};12\rangle + 0.43\,|\{(f\tfrac{7}{2})^3\}\tfrac{7}{2};12\rangle$$

$$|(\tfrac{3}{2}^-)_2\rangle = -0.48\,|\{(f\tfrac{7}{2})^2 0, p\tfrac{3}{2}\}\tfrac{3}{2};00\rangle - 0.30\,|\{(f\tfrac{7}{2})^2 2, p\tfrac{3}{2}\}\tfrac{3}{2};00\rangle$$
$$+0.31\,|\{(f\tfrac{7}{2})^2 0, p\tfrac{3}{2}\}\tfrac{3}{2};12\rangle - 0.28\,|\{(f\tfrac{7}{2})^3\}\tfrac{5}{2};00\rangle$$
$$+0.27\,|\{(f\tfrac{7}{2})^2 2, p\tfrac{3}{2}\}\tfrac{5}{2};12\rangle + 0.20\,|\{(f\tfrac{7}{2})^3\}\tfrac{7}{2};12\rangle$$
$$+0.24\,|\{(f\tfrac{7}{2})^2 2, p\tfrac{3}{2}\}\tfrac{7}{2};12\rangle - 0.21\,|\{(f\tfrac{7}{2})^3\}\tfrac{7}{2};24\rangle$$

$$|(\tfrac{5}{2}^-)_1\rangle = -0.25\,|\{(f\tfrac{7}{2})^2 2, p\tfrac{3}{2}\}\tfrac{3}{2};12\rangle + 0.48\,|\{(f\tfrac{7}{2})^3\}\tfrac{5}{2};00\rangle$$
$$-0.20\,|\{(f\tfrac{7}{2})^2 4, p\tfrac{3}{2}\}\tfrac{5}{2};00\rangle + 0.20\,|\{(f\tfrac{7}{2})^3\}\tfrac{5}{2};20\rangle$$
$$+0.47\,|\{(f\tfrac{7}{2})^3\}\tfrac{7}{2};12\rangle + 0.21\,|\{(f\tfrac{7}{2})^2 6, p\tfrac{3}{2}\}\tfrac{9}{2};12\rangle$$

$$|(\tfrac{7}{2}^-)_1\rangle = -0.29\,|\{(f\tfrac{7}{2})^3\}\tfrac{5}{2};12\rangle + 0.60\,|\{(f\tfrac{7}{2})^3\}\tfrac{7}{2};00\rangle$$
$$-0.30\,|\{(f\tfrac{7}{2})^3\}\tfrac{11}{2};12\rangle$$

$$|(\tfrac{11}{2}^-)_1\rangle = 0.49\,|\{(f\tfrac{7}{2})^3\}\tfrac{7}{2};12\rangle - 0.47\,|\{(f\tfrac{7}{2})^3\}\tfrac{11}{2};00\rangle$$
$$+0.24\,|\{(f\tfrac{7}{2})^2 6, p\tfrac{3}{2}\}\tfrac{11}{2};00\rangle + 0.27\,|\{(f\tfrac{7}{2})^3\}\tfrac{15}{2};12\rangle$$

$\mu(\frac{3}{2}_1^-) = 0.610\ \mu_N$, $\mu(\frac{11}{2}_1^-) = -1.223\ \mu_N$, and $\mu(\frac{3}{2}_2^-) = -0.707\ \mu_N$. The difference between these last values and those listed in Table VI stems from the collective part of the $\mathcal{M}(M1)$ operator.

The $\frac{7}{2}_1^- \rightarrow \frac{5}{2}_1^-$ and $\frac{5}{2}_1^- \rightarrow \frac{3}{2}_1^-$ $M1$ transitions are of the type $(j^3)J \rightarrow (j^3)J_1 \neq J$ and, therefore, exactly forbidden. On the other hand, the $\frac{5}{2}_1^- \rightarrow \frac{3}{2}_2^-$ and $\frac{3}{2}_1^- \rightarrow \frac{3}{2}_2^-$ $M1$ transitions are $l$ forbidden. Owing to the incoherence of the higher order effects these shell-model features are conserved in the exact calculation. The last transition arises mainly from the admixture of the $|\{(f_{7/2})^2 0, p_{3/2}\}\frac{3}{2},00;\frac{3}{2}\rangle$ configuration in the wave functions of the $\frac{3}{2}_1^-$ and $\frac{3}{2}_2^-$ states. With the above mentioned selection rules operating, the collective contributions, although small, are quite significant. In such a situation some additional higher order effects, for example, velocity dependent potentials,[54] might also be important.

The overall agreement between the theory and experiment for the electromagnetic properties is satisfactory (see Table VI), although we have no free parameters in order to fit the data (parametrization I). The calculations of the electromagnetic properties performed with the remaining three parametrizations, shown in Table I, yield quite similar results; owing to this fact, we do not present the corresponding results.

## IV. SUMMARY AND CONCLUSIONS

The properties of $N=85$ nuclei were calculated within the framework of the three-particle cluster-phonon coupling model. All available data on the low-lying states in $^{143}$Ce, $^{145}$Nd, $^{147}$Sm, and $^{149}$Gd nuclei were examined. With the parameters extracted in a simple way directly from experiment (parametrization I) it was possible to give a reasonable description of the electric and magnetic moments, the $B(E2)$ and $B(M1)$ values, and the spectroscopic amplitudes of the low $\frac{7}{2}_1^-$, $\frac{5}{2}_1^-$, $\frac{3}{2}_1^-$, $\frac{11}{2}_1^-$, and $\frac{3}{2}_2^-$ states. The energy spectra of the above mentioned nuclei, and, in particular, the energy splittings between the states of the triplet $\frac{7}{2}_1^-$, $\frac{5}{2}_1^-$, $\frac{3}{2}_1^-$ are also easy to understand within the CVM.

In order to account for the one-particle spectroscopic strengths in the energy region between 0.6 and 1.5 MeV, which were measured in $^{143}$Ce and $^{145}$Nd, it was necessary to significantly modify the

TABLE VI. Comparison of the calculated electromagnetic observables with the available experimental information for $N=85$ nuclei. The magnetic dipole and electric quadrupole moments are in units of $\mu_N$ and $e$ b, respectively. The $B(E2)$ and $B(M1)$ values are in units of $(e\text{ b})^2$ and $\mu_N{}^2$, respectively.

| | $^{145}$Nd | $^{147}$Sm | Experiment |
|---|---|---|---|
| $Q(\frac{7}{2}_1^-)$ | $-0.25$[a] | $-0.18$[b] | $-0.36$ |
| $Q(\frac{5}{2}_1^-)$ | | $-0.31\pm0.12$[b] | $-0.20$ |
| $Q(\frac{3}{2}_1^-)$ | | | 0.32 |
| $Q(\frac{11}{2}_1^-)$ | | | $-0.41$ |
| $Q(\frac{3}{2}_1^-)$ | | | $-0.30$ |
| $\mu(\frac{7}{2}_1^-)$ | $-0.654\pm0.004$[a] | $-0.813$[b] | $-0.794$ |
| $\mu(\frac{5}{2}_1^-)$ | | $-0.45$[b] | $-0.506$ |
| $\mu(\frac{3}{2}_1^-)$ | | $-0.30\pm0.10$[b] | $-0.698$ |
| $\mu(\frac{11}{2}_1^-)$ | | | $-0.822$ |
| $\mu(\frac{3}{2}_2^-)$ | | | $-0.658$ |
| $B(E2;\frac{7}{2}_1^-\rightarrow\frac{5}{2}_1^-)$ | | 0.093±0.011[c] | 0.112 |
| $B(E2;\frac{7}{2}_1^-\rightarrow\frac{3}{2}_1^-)$ | | 0.051±0.004[c] | 0.071 |
| $B(E2;\frac{7}{2}_1^-\rightarrow\frac{11}{2}_1^-)$ | | 0.191±0.007[c] | 0.186 |
| $B(E2;\frac{7}{2}_1^-\rightarrow\frac{3}{2}_1^-)$ | | 0.019±0.005[c] | 0.003 |
| $B(E2;\frac{5}{2}_1^-\rightarrow\frac{3}{2}_1^-)$ | | | 0.070 |
| $B(E2;\frac{5}{2}_1^-\rightarrow\frac{3}{2}_1^-)$ | | | 0.051 |
| $B(E2;\frac{3}{2}_1^-\rightarrow\frac{3}{2}_2^-)$ | | | 0.032 |
| $B(M1;\frac{7}{2}_1^-\rightarrow\frac{5}{2}_1^-$ | | 0.010[d] | 0.016 |
| $B(M1;\frac{5}{2}_1^-\rightarrow\frac{3}{2}_1^-)$ | | 0.001[d] | 0.008 |
| $B(M1;\frac{5}{2}_1^-\rightarrow\frac{3}{2}_2^-)$ | | | 0.013 |
| $B(M1;\frac{3}{2}_1^-\rightarrow\frac{3}{2}_2^-)$ | | | 0.047 |

[a]Reference 9.
[b]Reference 12.
[c]Reference 14.
[d]Reference 52.

"experimental" single-particle energies. We believe that this difference is a consequence of the truncation of the configuration space which we were forced to introduce due to practical reasons (i.e., to keep the maximum dimensions of the energy matrices within our computational possibilities). The work of Vanden Berghe and Paar[17] also supports this assumption. For the same reason, we have restricted the discussion to the low-lying negative parity states. One possible way to overcome the problem could be to extend the shell-model method of Liotta *et al.*[55,56] to the particle phonon model. Their formalism allows for drastic truncations in the configuration space, still giving states very close to the exact ones.

There is, evidently, considerable scope for more experimental work and theoretical analysis of the $N=85$ nuclei.

## ACKNOWLEDGMENTS

The authors are indebted to Dr. J. L. Foster, Jr. for many fruitful discussions as well as for use of experimental data prior to publication. F. K. is a member of the Carrera de Investigador Científico, Consejo Nacional de Investigacion Cientifica y Tecnológica, Argentina and was sponsored by Financiadora de Estudos e Projetos, Brasil.

[1]P. Carlos, H. Beil, R. Bergére, A. Leprêtre, A. de Miniac, and A. Veyssiére, Nucl. Phys. A225, 171 (1974).
[2]K. Heyde, M. Waroquier, and H. Vincx, Phys. Lett. 57B, 429 (1975).
[3]G. Vanden Berghe, Z. Phys. A 272, 245 (1975).
[4]A. Bohr and B. R. Mottelson, K. Dan. Vidensk. Selsk. Mat. Fys. Medd. 27, No. 16 (1953).
[5]B. J. Raz, Phys. Rev. 114, 1116 (1959).
[6]G. Alaga, Bull. Am. Phys. Soc. 4, 359 (1959).
[7]L. S. Kisslinger and R. A. Sorensen, Rev. Mod. Phys. 35, 853 (1963).
[8]J. K. Tuli, Nucl. Data Sheets 25, 603 (1978), and references therein.
[9]J. K. Tuli, Nucl. Data Sheets 29, 533 (1980), and references therein.
[10]G. Løvhøiden, J. R. Lien, S. El-Kazza, J. Rekstad, C. Ellegaard, J. H. Bjerregaard, P. Knudsen, and P. Kleinheinz, Nucl. Phys. A339, 477 (1980).
[11]J. L. Foster, Jr., private communication.
[12]B. Harmatz and W. B. Ewbank, Nucl. Data Sheets 25, 113 (1978), and references therein.
[13]J. Kownacki, Z. Sujkowski, E. Hammaren, E. Liukkonen, M. Piiparinen, Th. Lindbland, H. Ryde, and V. Paar, Nucl. Phys. A337, 464 (1980).
[14]V. Paar, G. Vanden Berghe, C. Garret, J. R. Leigh, and G. D. Dragoulis, Nucl. Phys. A350, 139 (1980).
[15]G. E. Holland, Nucl. Data Sheets 19, 337 (1976), and references therein.
[16]C. Garret, J. R. Leigh, and G. D. Dracoulis, Nucl. Phys. A262, 135 (1976).
[17]G. Vanden Berghe and V. Paar, Z. Phys. A 294, 183 (1980).
[18]G. Alaga and G. Ialongo, Nucl. Phys. A97, 600 (1967).
[19]R. Almar, O. Civitarese, F. Krmpotić, and J. Navaza, Phys. Rev. C 6, 187 (1972).
[20]V. Paar, Phys. Lett. 39B, 466 (1972).
[21]V. Paar, Phys. Lett. 42B, 8 (1972).
[22]V. Paar, Nucl. Phys. A211, 29 (1973).
[23]R. Almar, O. Civitarese, and F. Krmpotić, Phys. Rev. C 8, 1518 (1973).
[24]O. Civitarese and F. Krmpotić, Nucl. Phys. A229, 133 (1974).
[25]G. Vanden Berghe, Z. Phys. 266, 139 (1974).
[26]V. Paar, Z. Phys. 271, 11 (1974).
[27]V. Paar, in *Problems of Vibrational Nuclei,* edited by G. Alaga, V. Paar, and L. Šips (North-Holland, Amsterdam, 1975), p. 15.
[28]V. Paar, Phys. Rev. C 11, 1432 (1975).
[29]V. Paar, in *Heavy-Ion, High-spin States and Nuclear Structure* (IAEA, Vienna, 1975), Vol. II, p. 179.
[30]V. Paar, Nuovo Cimento 33A, 99 (1976).
[31]S. M. Abecasis, O. Civitarese, and F. Krmpotić, Z. Phys. A 278, 309 (1976).
[32]V. Paar and B. K. S. Koene, Z. Phys. A 297, 203 (1976).
[33]V. Paar, V. Eberth, and J. Ebert, Phys. Rev. C 13, 2537 (1976).
[34]G. Vanden Berge, Nucl. Phys. A265, 479 (1976).
[35]G. Vanden Berge, Z. Phys. A 279, 223 (1976).
[36]V. Paar, J. S. Vieu, and Ch. Dionisio, Nucl. Phys. A284, 199 (1977).
[37]R. A. Meyer, K. V. Marsh, D. S. Brenner, and V. Paar, Phys. Rev. C 16, 417 (1977).
[38]A. Szanto de Toledo, M. N. Rao, O. Sala, and F. Krmpotić, Phys. Rev. C 16, 438 (1977).
[39]G. Vanden Berge, Z. Phys. A 281, 355 (1977).
[40]W. Boath and S. Wilson, Nucl. Phys. A247, 126 (1975).
[41]Z. Haratyn, J. Kownacki, J. Ludziejewski, Z. Sujkowski, L. E. de Geer, A. Kerek, and H. Ryde, Nucl. Phys. A276, 299 (1977).
[42]D. Eccleshall, M. J. L. Yates, and J. J. Simpson, Nucl. Phys. 78, 481 (1966).
[43]J. F. Lemming and S. Raman, Nucl. Data Sheets 10, 309 (1973).
[44]O. Hansen and O. Nathan, Nucl. Phys. 42, 197 (1963).
[45]J. Blonquist and S. Wahlborn, Ark. Fys. 16, 545 (1960).
[46]It can be seen from the results shown in Table II that both radial form factors depend significantly on the single-particle states. Consequently, assuming constant values for them, as is usually done, might be a rather crude approximation, especially when the intruder single-particle state from the upper oscillator shell has a pronounced effect on the low-lying states. This seems to be the case with the $1i_{13/2}$ neutron orbital in the nuclei with $N \gtrsim 82$. Clearly the correlations and the excitation modes not included in the present approach will renormalize the bare form factors given in Table II. However, it is not obvious at all that these effects would wash out completely the underlying shell structure.
[47]L. Lessard, S. Gales, and J. L. Foster, Jr., Phys. Rev. C 6, 517 (1972).
[48]D. L. Hillis, C. R. Bingham, D. A. McClure, N. S. Kendrick, Jr., J. C. Hill, S. Raman, J. B. Ball, and J. A. Harvey, Phys. Rev. C 12, 260 (1975).

[49]M. Ogawa, R. Broda, K. Zell, P. J. Daly, and P. Kleinheinz, Phys. Rev. Lett. 41, 289 (1978).

[50]P. Kleinheinz, R. Broda, P. J. Daly, S. Lunadi, M. Ogawa, and J. Blonquist, Z. Phys. A 290, 279 (1979).

[51]W. Oelert, J. V. Maher, D. A. Sink, and M. J. Spisack, Phys. Rev. C 12, 417 (1975).

[52]R. A. Belt, E. G. Funk, and J. W. Mihelich, Nucl. Phys. A175, 129 (1971).

[53]G. Alaga, F. Krmpotić, V. Paar, and L. Šips, Rudjer Bosković Institute Reports No. IRB-TP-7-70 and IRB-TP-4-73 (unpublished).

[54]G. Alaga, in *Cargese Lectures in Theoretical Physics,* edited by M. Lévy (Gordon and Breach, New York, 1968), Vol. II; in *Nuclear Structure and Nuclear Reactions, Proceedings of the International School of Physics, "Enrico Fermi", Course XI,* edited by M. Jean and R. A. Ricci (Academic, New York, 1969).

[55]R. J. Liotta and B. A. Silvestre-Brac, Nucl. Phys. A309, 301 (1978).

[56]J. P. Boisson, B. A. Silvestre, and R. J. Liotta, Nucl. Phys. A330, 307 (1979).